

# A novel method for generating a rectangular convex corner compensation structure in an anisotropic etching process

Zhang Han(张涵) and Li Weihua(李伟华)<sup>†</sup>

(Key Laboratory of MEMS of the Ministry of Education, Southeast University, Nanjing 210096, China)

**Abstract:** Detailed characteristics of three classical rectangular convex corner compensation structures on (100) silicon substrates have been investigated, and their common design steps are summarized. By combining the basic method of a silicon wet anisotropic etching process, a general method of generating compensation structures for a rectangular convex corner is put forward. This calls for the following two steps: define the topological field and fit some borderlines together into practical compensation patterns. The rules, which must be obeyed during this process, are summarized. By introducing this method, some novel compensation patterns for rectangular convex corner structures are created on both (100) and (110) substrates, and finally simulation results are given to prove this new method's validity and applicability.

**Key words:** rectangular convex corner compensation; anisotropic etching; general methodology

**DOI:** 10.1088/1674-4926/30/7/073003

**PACC:** 0750

**EEACC:** 2573

## 1. Introduction

Silicon anisotropic wet etching with KOH (potassium hydroxide) is an important technique for realizing most of the three-dimensional micro-structures in MEMS (micro electromechanical system) devices<sup>[1-4]</sup>. Convex corner undercutting during this process is undesired. Corner erosion leads to deformed rectangular structures, which will subsequently influence the device performance<sup>[5]</sup>. As the key for preventing corner undercutting, research into rectangular convex corner compensation is especially important.

Most of the existing studies in compensation structure were carried out on (100) silicon substrate. Compensation patterns, such as triangle, square, and  $\langle 100 \rangle$  bar<sup>[6-8]</sup>, have been employed to protect the desired right-angled corner, and they have become the three classical compensation methods that are still widely used nowadays. However, each individual compensation structure is independent<sup>[9]</sup>, and the common principle of constructing a compensation pattern is not clearly put forward. Additionally, compensation on (110) substrate is rarely reported.

In this work, we try to discover the compensation structures' essence through their different shaped appearances. The concept of topological field is introduced, and the rules to be obeyed when transforming the topological field into practical compensation patterns are developed. With this method, compensation patterns for rectangular convex corners on (100) substrates can be created both conventionally and innovatively, and it also works on  $\langle 110 \rangle$  oriented silicon wafers. The simulation results indicate that this method can generate compensation patterns for rectangular mesa structures on any silicon substrate effectively.

## 2. Compensation principles

Most of the present investigations of compensation methods concentrate on (100) substrate. That is because it is one of the most widely used substrates. In addition, the (100) plane is a natural surface of the silicon atom unit lattice. The intersecting lines between the (100) substrate and other planes can be easily determined. In addition, the non-etching plane (111) meets the (100) plane in the  $\langle 110 \rangle$  direction<sup>[10]</sup>, which happens to be the right-angled edge. This paper will start with the study of three classical compensation methods and expects to discover their essence to arrive at a general route to suitable compensation patterns.

### 2.1. Classical compensation structures on (100) substrates

Under the condition of a 30% wt. KOH solution, (311) emerges as the fast-etching plane and the non-etching plane is (111)<sup>[8]</sup>. The  $\langle 310 \rangle$  and  $\langle 110 \rangle$  directions are their intersecting lines with the substrate, respectively. Other (100) planes are perpendicular to the substrate.

The three classical compensation structures are known as triangle, square, and  $\langle 100 \rangle$  bar<sup>[6-8]</sup>, as shown in Fig. 1.

#### 2.1.1. Compensation with triangle

Triangle compensation is realized by adding a  $\langle 310 \rangle$  edged triangle mask layout to the exposed rectangular convex corner, as shown in Fig. 1(a). In order to obtain an accurate right-angled corner, the borders of the triangle have to approach the corner apex simultaneously, and the time they take must equal the designed etching time. So the distance between the right-angled apex and the  $\langle 310 \rangle$  borders needs to satisfy the relationship  $d/v_{\langle 310 \rangle} = H/v_{\langle 100 \rangle}$ . Here  $v$  stands for

<sup>†</sup> Corresponding author. Email: liwh@seu.edu.cn

Received 15 January 2009, revised manuscript received 24 February 2009

© 2009 Chinese Institute of Electronics

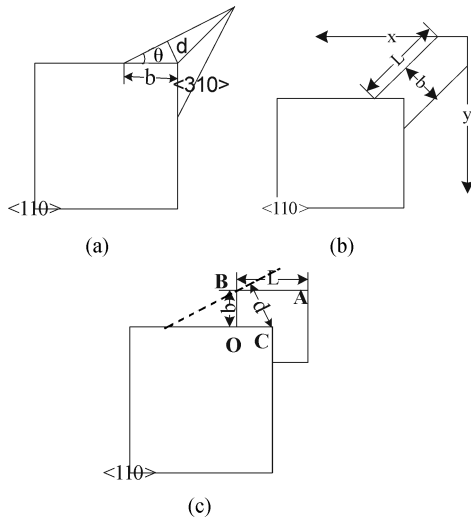


Fig. 1. Three classical compensation patterns: (a) Triangle; (b)  $\langle 100 \rangle$  bar; (c) Square.

velocity, and  $H$  is the etching depth. Considering the trigonometric function, the dimension is worked out as:  $b = \sqrt{5} \frac{v_{\langle 310 \rangle}}{v_{\langle 100 \rangle}} H^{[8]}$ .

### 2.1.2. $\langle 100 \rangle$ bar compensation

The traditional  $\langle 100 \rangle$  bar compensation adds the bar directly to the right-angled corner, as shown in Fig. 1(b). When the length of the bar is beyond some critical value, the  $\langle 100 \rangle$  side becomes the final cutting direction. Since the velocity of the  $\langle 100 \rangle$  plane is unique at same etching ambient, the width  $b$  of the bar should double the etching depth  $H$ . And the critical length  $L$  of the bar is proven to be equal to  $(1.581 \frac{v_{\langle 310 \rangle}}{v_{\langle 100 \rangle}} - 1) \times 2H^{[8]}$ .

### 2.1.3. Square compensation

Adding a  $\langle 110 \rangle$  edged square structure to the desired corner leads to the square compensation, as shown in Fig. 1(c). Undercutting also occurs at the convex corners of the compensation square itself. If  $OB = b$  and  $AB = L$ , the etching depth is still  $H$ , and the tangent value of the angle between  $\langle 310 \rangle$  and  $\langle 110 \rangle$  is 0.5. Draw a  $\langle 310 \rangle$  direction cross point B, and the distance  $d$  between the direction and point C is found to be  $3b/\sqrt{5}$ . When  $d$  and  $H$  satisfy  $d/v_{\langle 310 \rangle} = H/v_{\langle 100 \rangle}$ , the ideal compensation could just be realized, so we get  $b = \sqrt{5}Hv_{\langle 310 \rangle}/3v_{\langle 100 \rangle}^{[8]}$ .

### 2.1.4. Summary of the methods above

According to the compensation methods on the  $\langle 100 \rangle$  substrate mentioned above, we can draw the following conclusion:

- (1) All the right-angled edges are non-etching, so compensation is only for convex corner structures.
- (2) The fast-etching plane  $\langle 311 \rangle$  and the  $\langle 100 \rangle$  substrate intersect at  $\langle 310 \rangle$ , which dominates the undercutting.
- (3) When determining the dimensions of the compensation patterns, they used a similar mathematic equation:  $d/v = H/v_{\langle 100 \rangle}$ , where  $d$  stands for the distance from the desired apex

to the end-etching directions, which is across the farthest corner apex of the compensation pattern, and  $v$  is the end-etching direction's velocity.

## 2.2. General method for compensation

Although the three methods above have many common grounds, the practical compensation patterns are very different. By combining their common principles, we have developed a general method for generating compensation patterns. Firstly, define a topological field around the desired right-angled corner. Secondly, we follow some rules to form actual compensation structures from the topological field. Technically, this new approach of compensation patterns has great flexibility and adaptability.

The topological field can be defined by the following steps:

- (1) Identify the fast-etching planes and non-etching planes, and the velocity of them.
- (2) Determine the intersecting lines between the silicon substrate and the planes defined in step 1, and solve their two-dimensional etching rates.
- (3) Find out every fast-etching direction around the desired right-angled corner and make sure that the distance between them and the corner apex meets the relationship:  $d_{\text{fast-etching}}/v_{\text{fast-etching}} = H/v_{\text{substrate}}$ .
- (4) The largest boundary made by all these fast-etching directions composes the original topological field.

All the borders of the topological field share the distance to the desired corner apex. Concerning the truth that undercutting is dominated in fast-etching directions<sup>[11]</sup>, it is absolutely right to make compensation structures by directly selecting some borders under the condition that all the concave corners formed must be larger than the greatest angle between non-etching directions. While using other directions to construct the compensation patterns, every critical convex corner apex should be located on the topological boundary.

For some compensation structures, the end-etching direction is not the fast-etching side. The new chosen border has to meet the relation with the etching depth. The dimension of the chosen borderline may be beyond or within the original topological field, so the final profile of the compensation region will cause a complementary change.

We condense the description above into four general rules for generating compensation patterns from the topological field:

- (1) The convex corners of the compensation structure, whose undercutting directions are chosen as the end-etching directions, should be on the boundary of the topological field.
- (2) The angle of the convex corner defined in rule 1 shouldn't be larger than the fast-etching planes' angle.
- (3) The profile of the compensation pattern couldn't include any concave corners, unless they are made of two non-etching borders, or the concave corner is larger than the

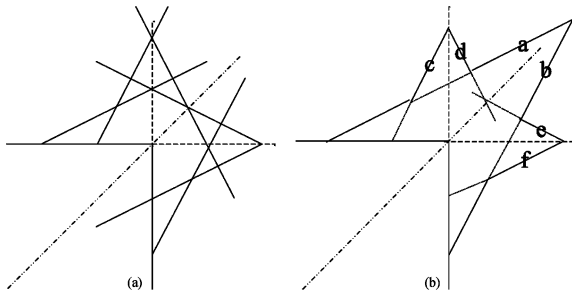


Fig. 2. Analysis of a right corner on a (100) substrate: (a)  $\langle 310 \rangle$  directions; (b) Topological field.

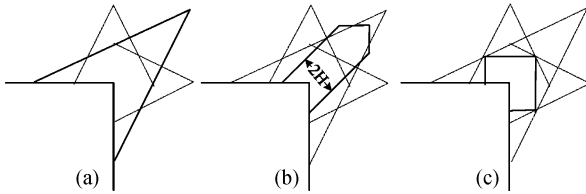


Fig. 3. Compensation patterns in Section 2.1 from the topological field: (a) Triangle; (b)  $\langle 100 \rangle$  bar; (c) Square.

angle contained by any two of the non-etching directions, and with one non-etching border.

(4) When taking some special crystal lines as the end-etching directions, we should take advantage of their characteristics to simplify the original design.

Obviously, rules 1, 2, and 3 are so important that every compensation structure has to meet them simultaneously. Rule 4 is complementary, and it is just for the case when not choosing the fast-etching line as the end-etching direction. The original topological field is the biggest extension for most compensation patterns. Actually, this field can be changed; once some borders' location changed, corresponding changes will cause other borders to keep the profile balance.

It's easy to apply this general method to researches of right-angled convex corner compensation on different kinds of substrates to test its flexibility and validity.

### 2.3. Theoretical analysis of rectangular convex corner compensation on (100) substrates

We still work on (100) substrate, trying to form some novel compensation patterns by using the general method.

According to Section 2.1, we have already known the properties of (100) substrate. All the  $\langle 310 \rangle$  directions around the right-angled corner are shown in Fig. 2(a), and the distance  $d$  between them and the apex meets the equation as:  $d/v_{\langle 310 \rangle} = H/v_{\langle 100 \rangle}$ . Figure 2(b) shows a clear view of the topological field with named borderlines.

All the three classical methods, i.e., triangle,  $\langle 100 \rangle$  bar, and square, can be generated from the topological field defined in Fig. 2(b). Figure 3 shows how this occurs.

From Fig. 3(a), the triangle compensation is made of lines  $a$  and  $b$ . The  $\langle 100 \rangle$  bar compensation is shown in Fig. 3(b). The width of the bar is twice the etching depth  $H$ . In order to cause  $\langle 100 \rangle$  to determine the final undercut, the apex of the  $\langle 100 \rangle$  sidewall is beyond the topological profile, and the

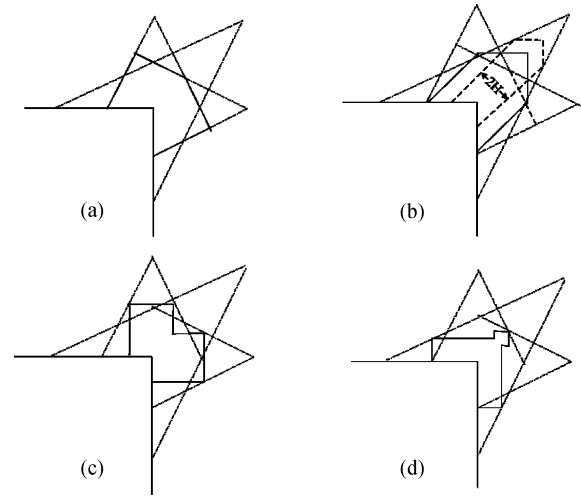


Fig. 4. Other compensation structures for a right-angled corner on a (100) substrate.

length is further than the intersection of lines  $d$  and  $e$ . In Fig. 3(c), every corner of the compensation square is on the intersection of two fast-etching directions to satisfy the rules.

Many novel compensation patterns can be created by choosing another line as the end-etching direction. The structure in Fig. 4(a) is made by the borders  $c$ ,  $e$ ,  $d$ , and  $f$ . In Fig. 4(b), the borders  $a$  and  $b$  are chosen to be the end-etching directions; so the apexes of the related corners must be on them, and the width of the compensation bar is wider than  $2H$  to make sure the  $\langle 100 \rangle$  side ends before  $\langle 310 \rangle$ . The length of the bar is beyond the intersecting point of the borders  $d$  and  $e$  to make directions  $a$  and  $b$  the only pair of end-etching directions. Figures 4(c) and 4(d) are distortions of the square compensation; both of them are according to the rules.

Apparently, with the restriction of the pattern generating rules, the topological field can be transformed into many different compensation structures besides the seven patterns mentioned above.

### 2.4. Theoretical analysis of rectangular convex corner compensation on a (110) substrate

As we know, the velocity of each crystal plane under the same etching conditions is unique<sup>[1,2]</sup>. The differences among different silicon substrates come from the included angle and the intersecting lines between the essential planes and the substrate.

Initially, on the (110) substrate, we identify the directions of the lines formed by intersecting the substrate itself with the non-etching and fast-etching planes. According to some experimental results<sup>[12]</sup>, (110) substrate crosses the (311) plane at direction  $\langle 332 \rangle$ , and as another fast-etching plane, (110) meets itself at  $\langle 100 \rangle$  and  $\langle 111 \rangle$ . Figure 5(a) shows their relative positions with detailed dimensions. Clearly, direction  $\langle 332 \rangle$  is within the boundary of  $\langle 111 \rangle$ ; so the final profile of fast-etching directions is made up of directions  $\langle 111 \rangle$  and  $\langle 100 \rangle$ . The angles between the planes they belonged to and the surface are  $60^\circ$  and  $90^\circ$ , respectively. Meanwhile, the non-etch-

Table 1. Basic features of the etching environment and the silicon substrates.

Substrate		Velocity of some critical planes ( $\mu\text{m}/\text{min}$ )				Included angle between some planes and the substrates	
Face	Edge	(100)	(110)	(311)	(111)	(311)	(110)
(100)	$\langle 110 \rangle$	1	1.414	1.414	0	$72^\circ 27'$	$45^\circ / 90^\circ$
(110)	$\langle 100 \rangle$	1	1.414	1.414	0	$90^\circ$	$60^\circ / 90^\circ$

Table 2. Velocity of the fast-etching and the non-etching directions.

Substrate		Velocity of some critical directions on the substrates ( $\mu\text{m}/\text{min}$ )				
Face	Edge	$\langle 100 \rangle$	$\langle 110 \rangle$	$\langle 310 \rangle$	$\langle 111 \rangle$	$\langle 211 \rangle$
(100)	$\langle 110 \rangle$	1	0	1.484	—	—
(110)	$\langle 100 \rangle$	1.414	0	—	1.632	0

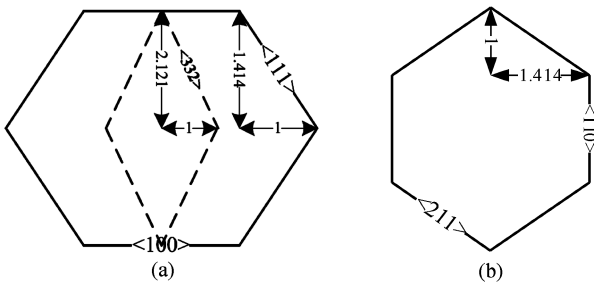


Fig. 5. Typical intersecting lines on a (110) substrate: (a) Fast-etching directions; (b) Non-etching directions.

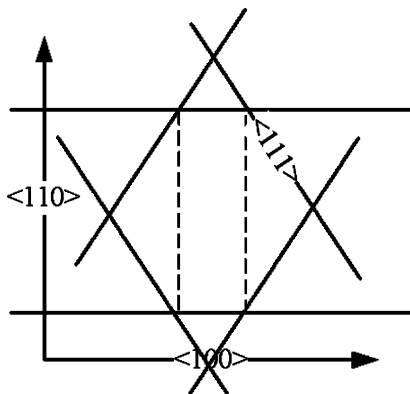


Fig. 6. Fast-etching directions around a rectangle.

ing plane (111) meets the (110) substrate at  $\langle 211 \rangle$  and  $\langle 110 \rangle$ , and their dimensions are shown in Fig. 5(b).

We designate a geometric coordinate system on a (110) substrate by  $\langle 100 \rangle$  and  $\langle 110 \rangle$ , and then considering a rectangular structure as shown in Fig. 6. In order to obtain an accurate right-angled mesa structure, the compensation pattern should just vanish when the structure reaches the designed depth. Observing a single right-angled corner, we make the fast-etching directions  $\langle 100 \rangle$  and  $\langle 111 \rangle$  to be a certain distance  $d$  away from the apex. The distance  $d$  and the etching depth  $H$  need to satisfy the relation:  $H/v_{(110)} = d_{(100)}/v_{(100)} = d_{(111)}/v_{(111)}$ . The final topological profile is shown in Fig. 7.

Since the  $\langle 100 \rangle$  direction overlaps with the horizontal edges, the line  $a$  is the only compensation borderline for an  $\langle 100 \rangle$  edge. The rest of the borders of the compensation pattern may be any other suitable direction depending on the design rules summarized in Section 2.2. Some possible compensation patterns are shown in Fig. 8.

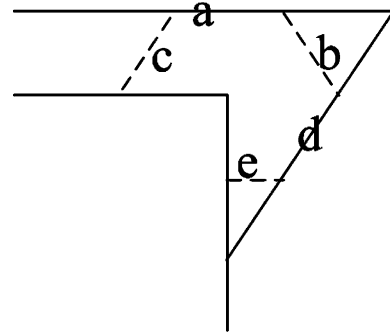


Fig. 7. Topological field around a right-angled corner.

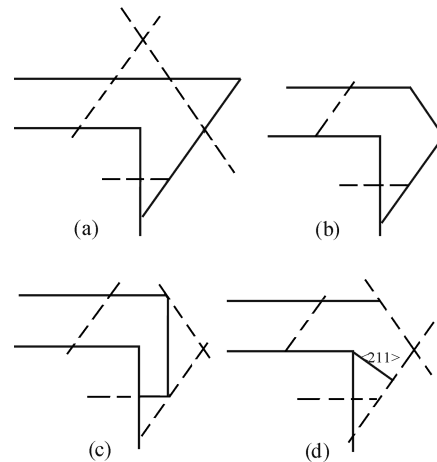


Fig. 8. Some compensation patterns for a right-angled corner on a (110) substrate.

The compensation structure in Fig. 8(a) chooses lines  $a$  and  $d$  to complete the boundary. Figure 8(b) adds the border  $b$  to the pattern of Fig. 8(a). Figure 8(c) is made up of borders  $a$ ,  $e$ , and another direction  $\langle 110 \rangle$  with every apex on the topological boundary. Figure 8(d) uses a non-etching direction  $\langle 211 \rangle$ , which forms a concave corner with the edge  $\langle 110 \rangle$ , but is still within the definition of the rules.

### 3. Simulation results

The simulation process started in a 30% wt. KOH solution at  $70^\circ\text{C}$ . Table 1 gives the basic features of the etching environment and the silicon substrates. Table 2 shows the velocity of the fast-etching and the non-etching directions on the substrates, which are calculated based on the information in

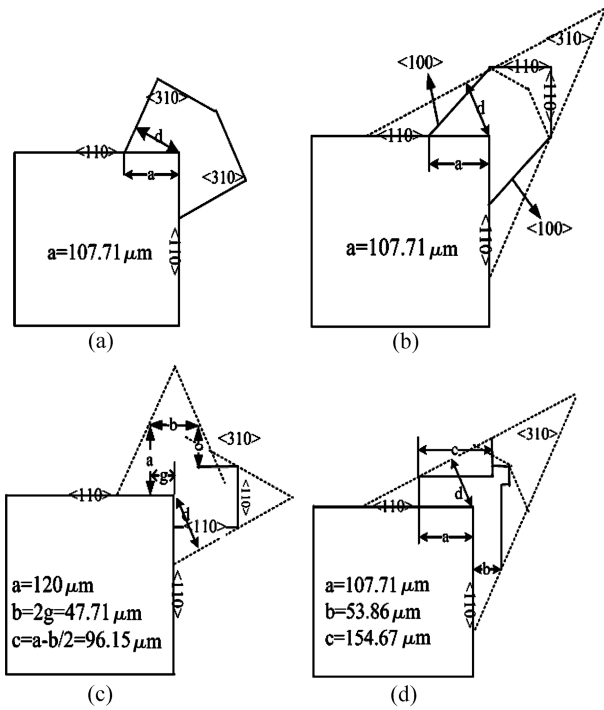


Fig. 9. Mask layouts on a (100) substrate with detailed dimensions.

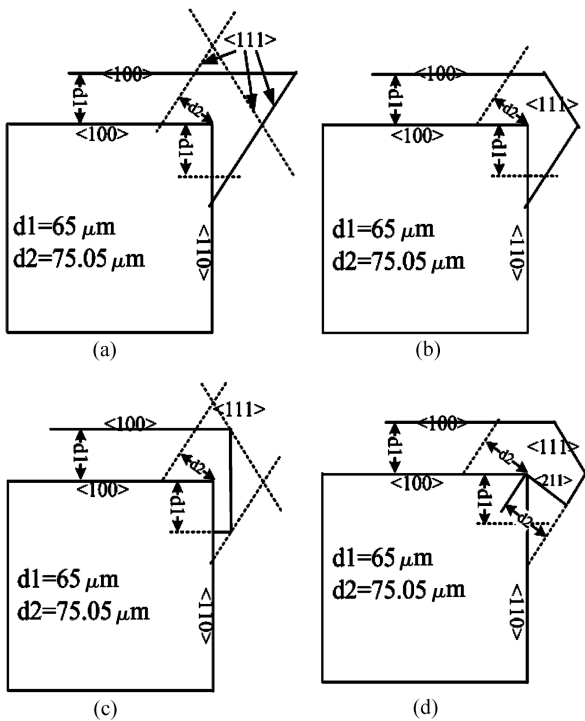


Fig. 10. Mask layouts on a (110) substrate with detailed dimensions.

Table 1.

In order to get a mesa structure of  $300 \times 300 \times 65 \mu\text{m}^3$ , the mask layouts designed in Sections 2.3 and 2.4 are given in Figs. 9 and 10, respectively, with detailed dimensions. The square side length is  $300 \mu\text{m}$ . The distance  $d$  from the right-angled corner apex to every  $\langle 310 \rangle$  direction on a (100) substrate is figured out to be  $96.3 \mu\text{m}$ . On a (110) substrate, the distance  $d_1$  from the apex to the direction  $\langle 100 \rangle$  is proved to be  $65 \mu\text{m}$ , while the distance  $d_2$  to the direction  $\langle 111 \rangle$  is  $75.05 \mu\text{m}$ .

The simulation of the mask layouts defined in Figs. 9

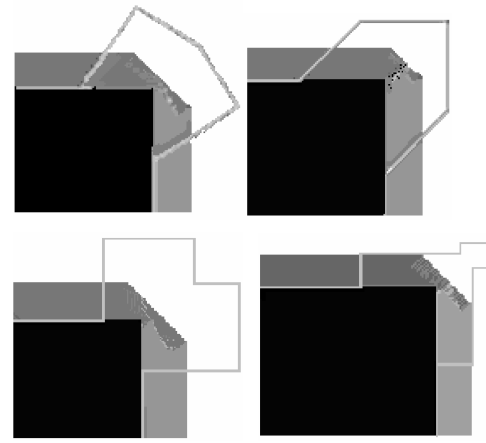


Fig. 11. Simulation results of the compensation patterns in Fig. 9.

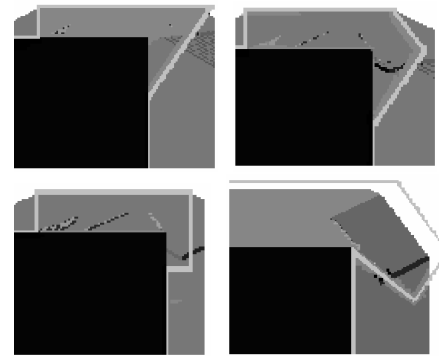


Fig. 12. Simulation results of the compensation patterns in Fig. 10.

and 10 were carried out by using an ACES (anisotropic crystalline etch simulation) tool. The simulation time designed on the (100) substrate and on the (110) substrate are 65 and 46 min, respectively.

Figure 11 shows the simulation results of the compensation patterns on a (100) substrate. Under the protection of these added mask layouts, it is clear that all the right-angled corners are completely formed. The simulation results of the patterns on the (110) substrate are shown in Fig. 12. Obviously, these results coincide with our expectations. Corners and edges with compensation patterns are perfectly preserved.

#### 4. Conclusion

A detailed investigation of the three classical compensation structures has been carried out to study the common essentials of generating suitable compensation patterns. The methodology we have summarized is easy and flexible, and it works very well on both (100) and (110) substrates.

The topological field is defined by the fast-etching directions, which are some certain distances away from the rectangular corner apex. The field can be changed. The pattern-producing rules manage the process of constructing an ideal compensation pattern from the topological field. They supplement and restrict each other, and maintain an internal balance.

This compensation method for rectangular corners depends upon the fundamental features of a wet anisotropic etching process. With precise technological parameters, it can cre-

ate novel compensation patterns without doing experiments first. The simulation results we gained above verify its validity and applicability. Moreover, it is convenient for realizing DFM (design for manufacture) in a MEMS design process.

## References

- [1] Seidel H, Csepregi L, Heuberger A. Anisotropic etching of crystalline silicon in alkaline solutions. *J Electrochem Soc*, 1990, 137(11): 3612
- [2] Glembocki O J, Palik E D, de Guel G R. Hydration model for the molarity dependence of the etch rate of Si in aqueous alkali hydroxides. *J Electrochem Soc*, 1991, 140(4): 1055
- [3] Barycka I, Zubel I. Silicon anisotropic etching in alkali solutions. *Sensors and Actuators*, 1998, 70: 250
- [4] Seidel H. The mechanism of anisotropic silicon etching and its relevance for micromachining. *Tech Dig Transducers*, Tokyo, Japan, 1987:120
- [5] Wu X P, Ko W H. Compensating corner undercutting in anisotropic etching of (100) silicon. *Sensors and Actuators*, 1989, 18: 207
- [6] Mayer G K, Offereings H L, Sandmaier H. Fabrication of nonunderetched convex corners in anisotropic etching of (100) silicon in aqueous KOH with respect to novel micromechanic elements. *J Electrochem Soc*, 1990, 137(12): 3947
- [7] Offereins H L, Kühl K, Sandmaier H. Methods for fabrication of convex corners in anisotropic etching of (100) silicon in aqueous KOH. *Sensors and Actuators*, 1990, A25: 9
- [8] Guo T, Fan B, Guo H. Convex corner compensation in anisotropy etching on silicon (100). *Nanotechnology and Precision Engineering*, 2008, 6: 68
- [9] Fan W, Zhang D. A simple approach to convex corner compensation in anisotropic KOH etching on a (100) silicon wafer. *J Micromech Microeng*, 2006, 16: 1951
- [10] Zhang P J, Huang Q A. Simulation of anisotropic etching of silicon based on MATLAB. *Journal of Semiconductors*, 2002, 23: 440
- [11] Huang Q A. *Silicon micromachining technology*. Beijing: Science Publisher, 1996
- [12] Than O, Buttgenbach S. Simulation of anisotropic chemical etching of crystalline silicon using a cellular automata model. *Sensors and Actuators*, 1994, 45(1): 85